

1 **Responses of coastal sediment organic and inorganic carbon**
2 **to habitat modification across a wide latitudinal range in**
3 **southeastern China**

4 Yan Hong^{a,b}, Linhai Zhang^{a,b,c}, Ping Yang^{a,b,c*}, Chuan Tong^{a,b,c}, Yongxin Lin^{a,b,c},
5 Derrick Y. F. Lai^d, Hong Yang^{e,f}, Yalian Tian^{a,b}, Wanyi Zhu^{a,b}, Kam W. Tang^{g*}

6 ^a*School of Geographical Sciences, Fujian Normal University, Fuzhou 350007, P.R.*
7 *China,*

8 ^b*Key Laboratory of Humid Subtropical Eco-geographical Process of Ministry of*
9 *Education, Fujian Normal University, Fuzhou 350007, P.R. China*

10 ^c*Research Centre of Wetlands in Subtropical Region, Fujian Normal University, Fuzhou*
11 *350007, P.R. China*

12 ^d*Department of Geography and Resource Management, The Chinese University of*
13 *Hong Kong, Shatin, New Territories, Hong Kong SAR, China*

14 ^e*College of Environmental Science and Engineering, Fujian Normal University, Fuzhou,*
15 *350007, China*

16 ^f*Department of Geography and Environmental Science, University of Reading,*
17 *Reading, RG6 6AB, UK*

18 ^g*Department of Biosciences, Swansea University, Swansea SA2 8PP, U. K.*

19

20 ***Correspondence to:**

21 Ping Yang (yangping528@sina.cn); Kam W. Tang (k.w.tang@swansea.ac.uk)

22 **Telephone:** 086-0591-87445659 **Fax:** 086-0591-83465397

23 **ABSTRACT**

24 Coastal wetlands are important to the global carbon (C) budget and climate regulation.
25 Plant invasion and aquaculture reclamation have drastically transformed China's
26 coastal wetlands, but knowledge of the effects on sediment carbon remains limited. We
27 sampled top layer sediments (0–20 cm) in 21 coastal wetlands in southeastern China
28 across the tropical-subtropical climate gradient, that have experienced the same
29 sequence of habitat transformation from native mudflats (MFs) to *Spartina alterniflora*
30 marshes (SAs) then to aquaculture ponds (APs). We measured the sediment carbon
31 contents and ancillary physicochemical parameters. Landscape change from MFs to
32 SAs increased sediment organic carbon (SOC) but decreased sediment inorganic
33 carbon (SIC) content, whereas conversion of SAs to APs resulted in the opposite
34 changes. Based on stepwise regression analysis, ammonium concentration and particle
35 size distribution were the common factors that affected changes in SOC between
36 habitat types, whereas for SIC it was ammonium and chloride concentrations. Habitat
37 change affected SOC to a larger degree than SIC. Overall, invasion of MFs by SAs
38 increased total carbon storage in the top sediment by 22%, or 6.6×10^6 g C ha⁻¹;
39 conversion of SAs to APs decreased it by 9.7%, or 3.5×10^6 g C ha⁻¹. Our results
40 showed the differential effects of different habitat modification scenarios on the
41 sediment carbon pools and help assess how landscape-scale change affects terrestrial
42 carbon budget and emission in the context of global climate change.

43 *Keywords:* Sediment organic carbon (SOC); Sediment inorganic carbon (SIC); Coastal

44 wetland; Invasive plants; Aquaculture reclamation; Carbon storage

45 **1. Introduction**

46 Coastal wetlands, including mudflats, salt marshes and mangroves, are among the
47 most productive ecosystems that are highly efficient in sequestering and storing carbon
48 to mitigate climate change (Bertram et al., 2021; Macreadie et al., 2021; Xu et al., 2022;
49 Zhang et al., 2021a). Despite covering just 0.2% of the Earth's surface, coastal
50 wetlands globally store at least 44.6 Tg C yr⁻¹ (Chmura et al., 2003), contributing 50%
51 of carbon burial into the sediment (Duarte et al., 2013). However, plant invasion and
52 reclamation increasingly modify the ecological properties of coastal wetlands (Bu et al.,
53 2015; Davidson et al., 2018; Sun et al., 2015), and are estimated to have caused
54 degradation or habitat loss in 50% of the world's coastal wetlands (Barbier et al., 2011;
55 Yang and Yang, 2020). These habitat modifications can greatly alter the hydrological
56 conditions, redox environment, nutrient cycles, sediment properties, biodiversity and
57 overall ecosystem structure (Andretta et al., 2016; Dick and Osunkoya, 2000; Lin et al.,
58 2022; Liu et al., 2022; Piper et al., 2015), thereby affecting the wetlands' carbon
59 capture and storage capacities (Bu et al., 2015).

60 Coastal wetlands in China cover approximately 5.80×10⁶ ha in 2014 (Sun et al.,
61 2015), which have been profoundly changed by *Spartina alterniflora* invasion (An et
62 al., 2007). As a way to control the spread of *S. alterniflora* and increase land use for
63 food production, some of the *S. alterniflora* marshes were subsequently cleared and
64 converted into aquaculture ponds (Duan et al., 2020). Today, there is an estimated total
65 area of 5.46×10⁴ ha of *S. alterniflora* marshes (Liu et al., 2018) and 1.56×10⁶ ha of

66 aquaculture ponds (Duan et al., 2020), representing over a quarter of the native wetland
67 area. Such a vast extent of landscape modification can have significant ramifications on
68 sediment carbon content, but most research to-date has been focused on the effects on
69 sediment organic carbon (SOC) at the local scale (Bu et al., 2015; Liu et al., 2021;
70 Xiang et al., 2015; Xu et al., 2022; Wan et al., 2018; Wang et al., 2021), while little is
71 known about how sediment inorganic carbon (SIC) will respond to *S. alterniflora*
72 invasion and reclamation (Yang and Yang, 2020; Zhu et al., 2020), or how habitat
73 modification affects wetland SOC and SIC pools across the wider geographical and
74 environmental gradients. This knowledge gap leads to uncertainties in the assessment
75 of regional and global wetland carbon budget and its feedback on climate.

76 To fill this knowledge gap, three habitat types (native mudflats, *S. alterniflora*
77 marshes and aquaculture ponds) from 21 coastal wetlands spanning 20°42' N to 31°51'
78 N in mainland China were investigated to gain insights into the effects of habitat
79 modifications on sediment carbon contents. The primary objectives were to investigate
80 the responses of SOC and SIC pools to *S. alterniflora* invasion and aquaculture
81 reclamation, and to evaluate the main environmental factors influencing the SOC and
82 SIC contents in impacted coastal wetlands across the tropical-subtropical gradient in
83 southeastern China. The results will improve our understanding of how landscape
84 modifications affect the coastal wetland carbon cycle at the national scale.

85 **2. Materials and methods**

86 *2.1. Study areas and sediment sampling*

87 Twenty-one coastal wetlands in five Chinese provinces were selected for this study,
88 including Shanghai (SH), Zhejiang (ZJ), Fujian (FJ), Guangdong (GD), and Guangxi
89 (GX), across the tropical-to-subtropical climate gradient (20°42' N to 31°51' N; 109°11'
90 E to 122°11' E) (Figure 1) (Yang et al., 2022). The region is characterized by monsoon
91 climate with an annual average temperature of 11.0–23.0 °C and precipitation of
92 100–220 cm. Coastal wetlands across the five provinces cover an area of approximately
93 2.58×10^6 ha (Sun et al., 2015), and they all have been impacted by *S. alterniflora*
94 invasion and aquaculture reclamation. Currently, *S. alterniflora* marshes and
95 aquaculture ponds in the five provinces are estimated to cover 3.34×10^4 ha (Liu et al.,
96 2018) and 5.31×10^5 ha (Duan et al., 2020), respectively.

97 Three habitat types were selected at each location: native mudflats (MFs), marshes
98 with invasive *S. alterniflora* (SAs) and reclaimed aquaculture ponds (APs) (Yang et al.,
99 2022). Field sampling was conducted between December 2019 and January 2020. At
100 each location, three independent replicate plots were selected for MFs (or SAs), and the
101 upper 0–20 cm sediments were collected using a steel corer (1.5 m length, 5 cm internal
102 diameter). For APs, independent replicate ponds were selected at each location. Within
103 each pond, a transect extending ~30 m from the bank to the center was used for
104 sampling at three sites at 10 m intervals. As a result, a total of 189 sediment samples
105 (21 sampling sites \times 3 habitat types \times 3 plots (or ponds)) collected. All sediment
106 samples were stored at 4 °C until analyses in the laboratory.

107 2.2. Sediment physicochemical analyses

108 In the laboratory, the sediment samples were freeze-dried, homogenized and then
109 ground into a fine powder for physicochemical analyses (Lu, 2000; Gao et al., 2019).
110 Briefly, sediment pH was measured with a pH meter (Orion 868 pH meter, USA; a
111 1:2.5 soil/distilled water mixture), salinity (as NaCl) with a salinity meter (Eutech
112 Instruments-Salt6, USA; a 1:5 soil/distilled water mixture) and particle size distribution
113 with a Master Sizer 2000 Laser Particle Size Analyzer (Malvern Instruments, UK).
114 Sediment ammonium-nitrogen ($\text{NH}_4^+\text{-N}$) and nitrate-nitrogen ($\text{NO}_3^-\text{-N}$) were measured
115 with a flow injection analyzer (Skalar Analytical SAN⁺⁺, Netherlands). Sediment water
116 content (SWC, %) and bulk density (BD, g cm^{-3}) were measured according to Percival
117 and Lindsay (1997) and Yin et al. (2019), and sediment SO_4^{2-} and Cl^- were determined
118 following Chen and Sun (2020). The data on sediment physiochemical properties are
119 given in Table S1.

120 2.3. Analysis of carbon contents

121 Plant residues and stones were removed from the sediment samples before total
122 carbon (TC) and sediment organic carbon (SOC) measurements. A subsample (~50 g
123 fresh sediment) was freeze-dried, homogenized and ground to fine powder, and then
124 sifted through a 2-mm mesh for carbon content analysis (Yang et al., 2022a, 2022b).
125 Approximately 1 g of the freeze-dried sample was analyzed with a combustion analyzer
126 (Elementar Vario MAX CN, Germany) for TC. To measure SOC, approximately 3 g of
127 freeze-dried sample was screened, weighed, and extracted in 1 M hydrochloric acid
128 (HCl) solution for 24 hr to remove the inorganic carbon, then oven-dried at 60°C (Liu

129 [et al., 2017; Yang et al., 2022](#)), and subsequently analyzed with the combustion
130 analyzer (Elementar Vario MAX CN, Germany). The content of sediment inorganic
131 carbon (SIC) was calculated as the difference between the TC and SOC ([Zhu et al.,](#)
132 [2020](#)). Sediment carbon storage at 0–20 cm depth per hectare was calculated from the
133 measured carbon content and bulk density as ([Wang et al., 2018; Zhu et al., 2020](#)):

$$134 \quad C_{\text{storage}} = C_{\text{content}} \times \text{BD} \times 20 \quad (\text{Eq. 1})$$

135 where C_{storage} is the carbon storage of TC, SOC or SIC at the 0–20 cm depth ($\times 10^6$ g C
136 ha^{-1}), C_{content} is the carbon content of TC, SOC or SIC (g kg^{-1}), and BD is the bulk
137 density (g cm^{-3}).

138 *2.4. Statistical analysis*

139 One-way analysis of variance (ANOVA) was conducted to test for significant
140 differences between habitat types for SOC, SIC and sediment physicochemical
141 properties, using the SPSS version 22.0 (IBM, Armonk, NY, USA). Spearman
142 correlation analysis was conducted to examine the relationships between SOC, SIC and
143 different sediment physicochemical variables, using corrplot and Hmisc packages in R
144 software (Version 4.1.0). The main variables influencing sediment SOC (or SIC)
145 content were evaluated by a stepwise regression analysis, and the results were plotted
146 using OriginPro 2021. The weighted response ratios (RR_{++}) were calculated to assess
147 the responses of SOC and SIC to habitat modification, following [Hedges et al. \(1999\)](#)
148 and [Tan et al. \(2019\)](#). All results were considered significant at $p < 0.05$ and were
149 presented as mean \pm 1 standard error.

150 **3. Results**

151 *3.1. SOC content across habitat types*

152 Across all sampling sites, the SOC content varied in the range of 1.87–9.35 g kg⁻¹
153 in MFs, 5.96–22.78 g kg⁻¹ in SAs, and 4.13–21.56 g kg⁻¹ in APs (Figure 2a). SOC
154 content (10.02 ± 0.54) was the highest in SAs (10.48 ± 0.95 g kg⁻¹), followed by APs
155 (8.48 ± 0.86 g kg⁻¹) and MFs (6.40 ± 0.43 g kg⁻¹) (Figure 2b). Based on the analysis of
156 weighted RR, conversion of MFs to SAs increased SOC content significantly by 70.9%,
157 but conversion of SAs to APs decreased SOC content by 15.3% (Figure 3a).

158 *3.2. SIC content across habitat types*

159 SIC content varied significantly in the range of 0.28–12.25 g kg⁻¹ (Figure 4a)
160 across habitat types ($p < 0.05$). SIC content was the highest in MFs (5.63 ± 0.49 g kg⁻¹),
161 followed by APs (4.63 ± 0.72 g kg⁻¹) and SAs (3.66 ± 0.50 g kg⁻¹) (Figure 4b). Based
162 on the analysis of weighted RR, conversion of MFs to SAs decreased SIC content
163 significantly by 33.6% (Figure 3b), but conversion of SAs to APs increased SIC content
164 by 26.9% (Figure 3b).

165 *3.3. Total carbon storage across habitat types*

166 Total C storage (TC_{storage}) in the top 0-20 cm sediment for the different habitat
167 types is shown in Figure 5. Across all sampling sites, TC_{storage} was the highest in SAs
168 (36.36 ± 1.57 × 10⁶ g C ha⁻¹), followed by APs (32.85 ± 1.59 × 10⁶ g C ha⁻¹) and MFs
169 (29.77 ± 0.75 × 10⁶ g C ha⁻¹) (Figure 5). TC_{storage} increased by 22.1% following the
170 conversion of MFs to SAs, but decreased by 9.7% when SAs were converted to APs.

171 SOC_{storage} was significantly higher than SIC_{storage} ($p<0.05$) and it accounted for
172 56.4–74.1 % of TC_{storage} (Figure 5).

173 3.4. Environmental control of sediment carbon contents

174 Spearman correlation analysis showed that in the case of MFs-to-SAs conversion,
175 SOC content was correlated positively with SWC, NH₄⁺-N and S_{clay} ($p<0.01$ or $p<0.001$)
176 and negatively with BD and S_{sand} ($p<0.01$ or $p<0.001$) (Figure 6a). SIC content was
177 correlated positively with S_{clay} and S_{silt} ($p<0.01$ or $p<0.001$) and negatively with salinity,
178 NH₄⁺-N and S_{sand} ($p<0.01$ or $p<0.001$) (Figure 6a).

179 In the case of SAs-to-APs conversion, SOC content was correlated positively with
180 NH₄⁺-N, Cl⁻, S_{clay} and S_{silt} ($p<0.01$ or $p<0.001$) and negatively with pH, SO₄²⁻ and S_{sand}
181 ($p<0.01$ or $p<0.001$) (Figure 6b). SIC content was correlated positively with S_{silt}
182 ($p<0.001$) and negatively with salinity, NH₄⁺-N, Cl⁻, SO₄²⁻ and S_{sand} ($p<0.01$ or $p<0.001$)
183 (Figure 6b).

184 Based on stepwise multiple regression analysis, NH₄⁺-N and pH were the main
185 drivers of SOC change in the case of MFs-to-SAs conversion, while SIC was mostly
186 influenced by NH₄⁺-N, sediment clay content, salinity and Cl⁻ (Table 1). Changes in
187 NH₄⁺-N, SO₄²⁻ and pH explained 43% of the variation in SOC in the case of
188 SAs-to-APs conversion, while SIC was strongly affected by Cl⁻, NH₄⁺-N, NO₃⁻-N and
189 SO₄²⁻ (Table 1).

190 4. Discussion

191 4.1. Habitat modification effect on sediment organic carbon

192 Although previous studies have evidenced that *S. alterniflora* invasion
193 significantly affected SOC content in vegetated wetlands in China (Li et al., 2009;
194 Xiang et al., 2015; Yang et al., 2017a; Zhang et al., 2021b), its effects on native
195 mudflats were less clear. Here, based on data from 21 coastal sites across the
196 tropical-subtropical gradient in China, we found that SOC content in the top 0-20 cm
197 SAs was significantly higher than that in MFs (Figure 2), representing an increase of
198 70.9% when native mudflats were converted to *S. alterniflora* marshes (Figure 3a).

199 The size of SOC pool in sediment is determined by the balance between organic
200 carbon inputs (autochthonous and allochthonous sources) and outputs (e.g.,
201 decomposition, leaching, removal, etc.) (Amundson, 2001; Hou et al., 2018;
202 Schlesinger and Bernhardt, 2013). The continuous river flow and periodic tidal flushing
203 in native mudflats would increase sediment erosion, reduce or dilute SOC and minimize
204 SOC accumulation in the sediment. Invasion by *S. alterniflora* could mitigate
205 sediment erosion by weakening water flow with aboveground biomass and stabilizing
206 the sediment with roots; it would also introduce more photosynthetically fixed carbon
207 into the sediment (Xiang et al., 2015; Yang et al., 2016; Zhang et al., 2010). We found
208 that $\text{NH}_4^+\text{-N}$ content in the SAs (24.0 g kg^{-1}) was higher than that in the MFs (13.3 g
209 kg^{-1}) (Figure 6a), likely reflecting the results of nutrient remineralization and retention
210 by the marsh vegetation (Liao et al., 2007; Yang and Guo, 2018). This higher level
211 $\text{NH}_4^+\text{-N}$ would support higher organic carbon production by plants and microbes
212 (Pastore et al., 2017; Xie et al., 2019; Wang et al., 2013), which would explain its

213 significant and positive correlation with SOC content ($p < 0.01$; Figure 6a).

214 Compared to coastal marshes, the deeper and stagnant nature of aquaculture pond
215 water would favor the development of anoxic condition within the sediment (Tan et al.,
216 2020; Yang et al., 2022b), which is expected to slow down the decomposition of
217 unconsumed feed and animal wastes and allow more organic matter to accumulate in
218 the sediment. However, we found that SOC in aquaculture ponds was significantly
219 lower than that in *S. alterniflora* marshes ($p < 0.001$; Figure 2b). In the aquaculture
220 ponds, organic carbon mainly came as external supply of feed, but most of which
221 would be converted to farmed animal biomass and be harvested from the ponds. In
222 contrast, organic carbon was mainly produced internally via photosynthesis in the
223 marshes, most of which would remain in the system (not harvested); hence, SOC was
224 able to accumulate to a higher level over time.

225 4.2. Habitat modification effect on sediment inorganic carbon

226 SIC plays an important role in C sequestration, especially in coastal
227 saline–alkaline areas (Zhu et al., 2020), but few studies have investigated the effect of
228 plant invasions and aquaculture reclamation on SIC in coastal wetland (Yang and Yang,
229 2020; Zhu et al., 2020). Here we showed that native mudflats had higher SIC than *S.*
230 *alterniflora* marshes (Figure 4b). The SIC pool consists mainly of carbonates, which
231 include lithogenic inorganic carbon (LIC) and pedogenic inorganic carbon (PIC). LIC is
232 derived from the parent sediment material, which is conserved in unweathered
233 sediments (Wu et al., 2009; Yang and Yang, 2020). PIC is formed by direct precipitation

234 of carbonate parent material (Eq. 2) (Wu et al., 2009; Yang and Yang, 2020) or
235 weathering of calcium silicate (Eq. 3) (Lal and Kimble, 2000; Emmerich, 2003; Wu et
236 al., 2009):



238 The processes can be driven by microbes in saline sediments (Dupraz et al., 2004;
239 Kremer et al., 2008; Schlager, 2003), especially photosynthetic microbes (Zhu and
240 Dittrich, 2016). Dense vegetation in the marshes would have competed against benthic
241 autotrophs for nutrients and light, therefore decreased biological precipitation of PIC
242 when the mudflats were invaded by *S. alterniflora*.

243 The increase in SIC following conversion of *Spartina* marshes to aquaculture
244 ponds might be related to management practices. For example, addition of fertilizer in
245 the form of NH_4HCO_3 would have favored carbonate precipitation, as has been shown
246 in the conversion of coastal marshes to croplands (Zhu et al., 2020). Also, liming was
247 used by some farmers to disinfect the ponds prior to stocking (Pouil et al., 2019; Yang
248 et al., 2022b), which would have increased sediment Ca^{2+} concentration and promoted
249 SIC formation.

250 4.3. Implications for sediment carbon storage and emission

251 In the literature, the response of coastal sediment C storage to landscape change
252 varied markedly. Zhu et al. (2020) found that conversion of coastal marshes to
253 croplands decreased total C storage ($\text{TC}_{\text{storage}}$) in the top sediment (0–15 cm) by
254 21–52%. Wang et al. (2019) showed that $\text{TC}_{\text{storage}}$ increased by 8% following the

255 conversion of *Phragmites australis* marshes to *S. alterniflora* marshes, while
256 conversion of mangrove marshes to *S. alterniflora* marshes decreased TC_{storage} by 18%.
257 [Xia et al. \(2021\)](#) reported that *S. alterniflora* invasion decreased SOC storage in
258 mangrove marshes dominated by *Kandelia obovata* and *Avicennia marina* but it had no
259 effect in *P. australis* saltmarshes across the tropical and subtropical regions of coastal
260 China. Conversely, [Xu et al. \(2022\)](#) found that *S. alterniflora* invasion had no
261 significant effect on SOC storage in vegetated native wetlands in coastal China. The
262 highly variable and at times conflicting observations suggest that the response of
263 sediment C storage may depend on the local environmental conditions as well as the
264 scenario of habitat change. To attain a better understanding of the topic, we sampled 21
265 coastal wetlands that spanned a broad geographical and climate gradient, and that have
266 undergone the same sequence of transformation, i.e., from mudflats to *S. alterniflora*
267 marshes then to aquaculture ponds.

268 *Spartina alterniflora* was introduced to China over 4 decades ago to restore coastal
269 vegetation, provide biofuel material, protect and stabilize shoreline ([Zhang et al., 2017](#)),
270 but it has since spread rapidly throughout China's coasts ([An et al., 2007](#)). While
271 invasion of mudflats by *S. alterniflora* has negative impacts on coastal flora and fauna
272 ([Chen et al., 2004](#); [Li et al., 2009](#)), based on our findings, it also significantly increased
273 TC_{storage} by 22.1% in the top 0–20 cm sediment ([Figure 5](#)); along with the above-ground
274 biomass and deeper root mass, this represents a large increase in 'fixed' carbon in the
275 land. In the context of carbon capture and climate mitigation, this may be viewed as an

276 unintended benefit of *S. alterniflora* invasion.

277 As a measure to control the spread of *S. alterniflora* and to support coastal
278 aquaculture, increasingly more *Spartina* marshes are being cleared and converted to
279 aquaculture ponds (Duan et al., 2021). Based on our data, such habitat modification
280 would decrease TC_{storage} by 9.7% (Figure 5). As the coastal aquaculture sector in China
281 continues to expand (Ren et al., 2019), conversion of *Spartina* marshes to aquaculture
282 ponds would release a vast amount of stored carbon from the marsh sediment, adding to
283 the overall climate footprint of the aquaculture operation (Yuan et al., 2019).

284 Sediment carbon includes both SOC and SIC; interestingly, SOC and SIC
285 responded very differently to habitat modifications (Figure 3). Conversion of mudflats
286 to *Spartina* marshes increased SOC but decreased SIC; the opposite occurred when
287 *Spartina* marshes were converted to aquaculture ponds (Figure 3). Because SOC and
288 SIC likely have different chemical reactivity and susceptibility to microbial actions, the
289 different directions of change would affect the overall carbon dynamics in the sediment.
290 For example, some of the SOC could be metabolized by microbes under anoxic
291 condition into CH_4 , which has a stronger warming effect than CO_2 (Gao et al., 2018;
292 Tong et al., 2012; Xiang et al., 2015; Yang et al., 2017b). Therefore, the higher TC_{storage}
293 as well as higher proportion of SOC in marshes and aquaculture ponds make them
294 potentially stronger hotspots than mudflats to drive further warming.

295 **5. Conclusions and recommendations**

296 The coastal landscape of China has undergone significant transformation over the

297 past several decades. We showed that the sequence of change from native mudflats to
298 *Spartina* marshes to aquaculture ponds has resulted in significant changes to the
299 sediment C pool. Overall, invasion of mudflats by *S. alterniflora* increased C storage in
300 the top sediment by 6.6×10^6 g C ha⁻¹, which may help mitigate climate warming. On
301 the other hand, conversion of *Spartina* marshes to aquaculture ponds decreased the
302 sediment C storage by 3.5×10^6 g C ha⁻¹, which needs to be taken into account when
303 assessing the climate impact of the expanding coastal aquaculture sector.

304 Plant invasions and aquaculture reclamation affect not only sediment
305 physicochemical properties, but also various sediment microfauna. Novel methods such
306 as isotopic tracing can be used to quantify the microfauna's contribution to sediment C
307 pool, its stability and turnover. Likewise, process measurements such as microbial
308 metabolism will help understand and predict changes to the dynamics and fate of
309 sediment carbon. In this study, we estimated the landscape-scale change in sediment
310 carbon storage in response to habitat modifications. Our findings can be coupled with
311 GIS and process-based data to hind- and fore-cast landscape-scale change in coastal
312 sediment carbon dynamics and emission.

313

314 **Declaration of competing interest**

315 The authors declare that they have no known competing financial interests or
316 personal relationships that could have appeared to influence the work reported in this
317 paper.

318 **Acknowledgements**

319 This research was supported by the National Science Foundation of China (No.
320 41801070, 41671088), the National Science Foundation of Fujian Province (No.
321 2020J01136, 2019J05067).

322 **References**

- 323 Amundson, R., 2001. The carbon budget in soils. *Annua. Rev. Earth Pl. Sc.* 29,
324 535–562. <https://doi.org/10.1146/annurev.earth.29.1.535>
- 325 An, S.Q., Gu, B.H., Zhou, C.F., Wang, Z.S., Liu, Y.H., 2007. *Spartina* invasion in China:
326 implications for invasive species management and future research. *Weed Res.* 47(3),
327 183–191. <https://doi.org/10.1111/j.1365-3180.2007.00559.x>
- 328 Andreetta, A., Huertas, A.D., Lotti, M., Cerise, S., 2016. Land use changes affecting
329 soil organic carbon storage along a mangrove swamp rice chronosequence in the
330 Cacheu and Oio regions (northern Guinea-Bissau). *Agr. Ecosyst. Environ.* 216,
331 314–321. <https://doi.org/10.1016/j.agee.2015.10.017>
- 332 Barbier, E.B., Hacker, S.D., Kennedy, C., Koch, E.W., Stier, A.C., Silliman, B.R., 2011.
333 The value of estuarine and coastal ecosystem services. *Ecol. Monogr.* 81, 169–193.
334 <https://doi.org/10.1890/10-1510.1>
- 335 Bertram, C., Quaas, M., Reusch, T.B.H., Vafeidis, A.T., Wolff, C., Rickels, W., 2021.
336 The blue carbon wealth of nations. *Nat. Clim. Change* 11(8), 704–709.
337 <https://doi.org/10.1038/s41558-021-01089-4>
- 338 Bu, N.S., Qu, J.F., Li, G., Zhao, B., Zhang, R.J., Fang, C.M., 2015. Reclamation of
339 coastal salt marshes promoted carbon loss from previously-sequestered soil carbon
340 pool. *Ecol. Eng.*, 81, 335–339. <http://dx.doi.org/10.1016/j.ecoleng.2015.04.051>
- 341 Chen, B.B., Sun, Z.G., 2020. Effects of nitrogen enrichment on variations of sulfur in
342 plant-soil system of *Suaeda salsa* in coastal marsh of the Yellow River estuary.
343 China. *Ecol. Indic.* 109, 105797. <https://doi.org/10.1016/j.ecolind.2019.105797>
- 344 Chen, Z.Y., Li, B., Zhong, Y., Chen, J.K., 2004. Local competitive effects of introduced
345 *Spartina alterniflora* on *Scirpus mariqueter* at Dongtan of Chongming Island, the

346 Yangtze River estuary and their potential ecological consequences. *Hydrobiologia*
347 528, 99–106. <https://doi.org/10.1007/s10750-004-1888-9>

348 Davidson, I. C., Cott, G. M., Devaney, J. L., Simkanin, C., 2018. Differential effects of
349 biological invasions on coastal blue carbon: A global review and meta-analysis.
350 *Global Change Biol.* 24(11), 5218–5230. <https://doi.org/10.1111/gcb.14426>

351 Dick, T.M., Osunkoya, O.O., 2000. Influence of tidal restriction floodgates on
352 decomposition of mangrove litter. *Aquat. Bot.* 68, 273–280.
353 [https://doi.org/10.1016/S0304-3770\(00\)00119-4](https://doi.org/10.1016/S0304-3770(00)00119-4)

354 Duan, Y.Q., Li, X., Zhang, L.P., Chen, D., Liu, S.A., Ji, H.Y., 2020. Mapping
355 national-scale aquaculture ponds based on the Google Earth Engine in the Chinese
356 coastal zone. *Aquaculture* 520, 734666.
357 <https://doi.org/10.1016/j.aquaculture.2019.734666>

358 Duan, Y. Q., Tian, B., Li, X., Liu, D. Y., Sengupta, D., Wang, Y. J., et al. (2021).
359 Tracking changes in aquaculture ponds on the China coast using 30 years of
360 Landsat images. *Inter. J. Appl. Earth Obs.* 102, 102383.
361 <https://doi.org/10.1016/j.jag.2021.102383>

362 Duarte, C.N., Losada, I.J., Hendriks, I.E., Mazarrasa, I., Marbà, N., 2013. The role of
363 coastal plant communities for climate change mitigation and adaptation. *Nat. Clim.*
364 *Change* 3(11), 961–968. <https://doi.org/10.1038/nclimate1970>

365 Dupraz, C.P., Visscher, T., Baumgartner, L.K., Reid, R.P., 2004. Microbe–mineral
366 interactions: early carbonate precipitation in a hypersaline lake (Eleuthera Island,
367 Bahamas). *Sedimentology* 51, 745–765.
368 <https://doi.org/10.1111/j.1365-3091.2004.00649.x>

369 Emmerich, W.E., 2003. Carbon dioxide fluxes in a semiarid environment with high
370 carbonate soils. *Agr. Forest Meteorol.* 116, 91–102.
371 [https://doi.org/10.1016/S0168-1923\(02\)00231-9](https://doi.org/10.1016/S0168-1923(02)00231-9)

372 Gao, D.Z., Liu, M., Hou, L.J., Derrick, Y.F.L., Wang, W.Q., Li, X.F., Zeng, A.Y., Zheng,
373 Y.L., Han, P., Yang, Y., Yin, G.Y., 2019. Effects of shrimp-aquaculture reclamation
374 on sediment nitrate dissimilatory reduction processes in a coastal wetland of
375 southeastern China. *Environ. Pollut.* 255, 113219.
376 <https://doi.org/10.1016/j.envpol.2019.113219>

- 377 Gao, G.F., Li, P.F., Shen, Z.J., Qin, Y.Y., Zhang, X.M., Ghoti, K.,Z., Zhu, X.Y., Zheng,
378 H. L., 2018. Exotic *Spartina alterniflora* invasion increases CH₄ while reduces CO₂
379 emissions from mangrove wetland soils in southeastern China. *Sci. Rep.* 8, 9243.
380 <https://doi.org/10.1038/s41598-018-27625-5>
- 381 Hedges, L.V., Gurevitch, J., Curtis, P.S., 1999. The meta-analysis of response ratios in
382 experimental ecology. *Ecology* 80, 1150–1156. <https://doi.org/10.2307/177062>
- 383 Hou, L.L., Zou, Y.C., Lyu, X.G., Zhang, Z.S., Wang, X.H., An, Y., 2018. Effect of
384 wetland reclamation on soil organic carbon stability in peat mire soil around
385 Xingkai Lake in Northeast China. *Chinese Geogr. Sci.* 2018 28(2), 325–336.
386 <https://doi.org/10.1007/s11769-018-0939-5>
- 387 Kremer, B., Kazmierczak, J., Stal, L.J., 2008. Calcium carbonate precipitation in
388 cyanobacterial mats from sandy tidal flats of the North Sea. *Geobiology* 6(1), 46–56.
389 <https://doi.org/10.1111/j.1472-4669.2007.00128.x>
- 390 Lal, R.J., Kimble, J.M., 2000. *Pedogenic carbonates and the global carbon cycle*. In:
391 Lal, R., Kimble, J.M., Eswaran, H., Stewart, B.A. (Eds.), *Global Change and*
392 *Pedogenic Carbonate*. CRC Press, Boca Raton, FL, pp. 1–14.
- 393 Li, B., Liao, C.H., Zhang, X.D., Chen, H.L., Wang, Q., Chen, Z.Y., Gan, X.J., Wu, J.H.,
394 Zhao, B., Ma, Z.J., Cheng, X.L., Jiang, L.F., Chen, J.K., 2009. *Spartina alterniflora*
395 invasions in the Yangtze River estuary, China: an overview of current status and
396 ecosystem effects. *Ecol. Eng.* 35, 511–520.
397 <http://dx.doi.org/10.1016/j.ecoleng.2008.05.013>
- 398 Liao, C.Z., Luo, Y.Q., Jiang, L.F., Zhou, X.H., Wu, X.W., Fang, C.M., Chen, J.K., Li,
399 B., 2007. Invasion of *Spartina alterniflora* enhanced ecosystem carbon and nitrogen
400 stocks in the Yangtze Estuary, China. *Ecosystems* 10, 1351–1361.
401 <https://doi.org/10.1007/s10021-007-9103-2>
- 402 Lin, Q.W., Wang, S.S., Li, Y.C., Riaz, L., Yu, F., Yang, Q.X., Han, S.J., Ma, J.M., 2022.
403 Effects and mechanisms of land-types conversion on greenhouse gas emissions in
404 the Yellow River floodplain wetland. *Sci. Total Environ.* 813, 152406.
405 <http://dx.doi.org/10.1016/j.scitotenv.2021.152406>
- 406 Liu, J.E., Deng, D.L., Zou, C.Y., Han, R.M., Xin, Y., Shu, Z.H., Zhang, L.M., 2021.
407 *Spartina alterniflora* saltmarsh soil organic carbon properties and sources in coastal

408 wetlands. J. Soils Sediment. 21, 3342–3351.
409 <https://doi.org/10.1007/s11368-021-02969-0>

410 Liu, J.E., Han, R.M., Su, H.R., Wu, Y.P., Zhang, L.M., Richardson, C.J., Wang, G.X.,
411 2017. Effects of exotic *Spartina alterniflora* on vertical soil organic carbon
412 distribution and storage amount in coastal salt marshes in Jiangsu, China. Ecol.
413 Eng., 106, 132–139. <http://dx.doi.org/10.1016/j.ecoleng.2017.05.041>

414 Liu, J.Q., Wang, W.Q., Shen, L.D., Yang, Y.L., Xu, J.B., Tian, M.H., Liu, X., Yang,
415 W.T., Jin, J.H., Wu, H.S., 2022. Response of methanotrophic activity and
416 community structure to plant invasion in China’s coastal wetlands. Geoderma 407,
417 115569. <https://doi.org/10.1016/j.geoderma.2021.115569>

418 Liu, M.Y., Mao, D.H., Wang, Z.M., Li, L., Man, W.D., Jia, M.M., Ren, C.Y., Zhang,
419 Y.Z., 2018. Rapid invasion of *Spartina alterniflora* in the coastal zone of mainland
420 China: new observations from Landsat OLI images. Remote Sens. 10, 1933,
421 <http://dx.doi.org/10.3390/rs10121933>

422 Macreadie, P.I., Costa, M.D.P., Atwood, T.B., Friess, D.A., Kelleway, J.J., Kennedy, H.,
423 Lovelock, C.E., Serrano, O., Duarte, C.M., 2021. Blue carbon as a natural climate
424 solution. Nat. Rev. Earth Environ. 2(12), 826–839.
425 <https://doi.org/10.1038/s43017-021-00224-1>

426 Pastore, M.A., Megonigal, J.P., Langley, J.A., 2017. Elevated CO₂ and nitrogen
427 addition accelerate net carbon gain in a brackish marsh. Biogeochemistry 133,
428 73–87. <https://doi.org/10.1007/s10533-017-0312-2>

429 Percival, J., Lindsay, P., 1997. Measurement of physical properties of sediments. In:
430 [Mudrock, A., Azcue, J. M., & Mudrock, P. \(Eds.\), Manual of Physico-Chemical](#)
431 [Analysis of Aquatic Sediments. CRC Press, New York, USA, pp. 7–38.](#)

432 Piper, C.L., Siciliano, S.D., Winsley, T., Lamb, E.G., 2015. Smooth brome invasion
433 increases rare soil bacterial species prevalence, bacterial species richness and
434 evenness. J. Ecol. 103, 386–396. <https://doi.org/10.1111/1365-2745.12356>

435 Pouil, S., Samsudin, R., Slembrouck, J., Sihabuddin, A., Sundari, G., Khazaidan, K.,
436 Kristanto, A.H., Pantjara, B., Caruso, D., 2019. Nutrient budgets in a small-scale
437 freshwater fish pond system in Indonesia. Aquaculture 504, 267–274.

438 <https://doi.org/10.1016/j.aquaculture.2019.01.067>

439 Ren, C.Y., Wang, Z.M., Zhang, Y.Z., Zhang, B., Chen, L., Xia, Y.B., Xiao, X.M.,
440 Doughty, R.B., Liu, M.Y., Jia, M., Mao, D.H., Song, K.S., 2019. Rapid expansion
441 of coastal aquaculture ponds in China from Landsat observations during 1984–2016.
442 *Inter. J. Appl. Earth Obs.* 82, 101902. <https://doi.org/10.1016/j.jag.2019.101902>

443 Schlager, W., 2003. Benthic carbonate factories of the Phanerozoic. *Int. J. Earth Sci.* 92,
444 445–464. <http://dx.doi.org/10.1007/s00531-003-0327-x>

445 Schlesinger, W.H., Bernhardt, E.S., 2013. Chapter 5-The biosphere: the carbon cycle of
446 terrestrial ecosystems. In: Schlesinger W H and Bernhardt E S (eds.).
447 *Biogeochemistry (Third Edition)*. Boston: Academic Press, 135–172.

448 Sun, Z.G., Sun, W.G., Tong, C., Zeng, C.S., Yu, X., Mou, X.J., 2015. China's coastal
449 wetlands: Conservation history, implementation efforts, existing issues and
450 strategies for future improvement. *Environ. Int.* 79, 25–41.
451 <http://dx.doi.org/10.1016/j.envint.2015.02.017>

452 Tan, L.S., Ge, Z.M., Zhou, X.H., Li, S.H., Li, X.Z., Tang, J.W., 2020. Conversion of
453 coastal wetlands, riparian wetlands, and peatlands increases greenhouse gas
454 emissions: A global meta-analysis. *Global Change Biol.* 26, 1638–1653.
455 <http://dx.doi.org/10.1111/gcb.14933>

456 Tong, C., Wang, W.Q., Huang, J.F., Gauci, V., Zhang, L.H., Zeng, C.S., 2012. Invasive
457 alien plants increase CH₄ emissions from a subtropical tidal estuarine wetland.
458 *Biogeochemistry* 111, 677–693. <https://doi.org/10.1007/s10533-012-9712-5>

459 Wang, J.B., Zhu, T.C., Ni, H.W., Zhong, H.X., Fu, X.L., Wang, J.F., 2013. Effects of
460 elevated CO₂ and nitrogen deposition on ecosystem carbon fluxes on the Sanjiang
461 Plain Wetland in Northeast China. *PLoS ONE* 8(6), e66563.
462 <https://doi.org/10.1371/journal.pone.0066563>

463 Wang, L., Yuan, J.H., Wang, Y., Butterly, C.R., Tong, D.L., Zhou, B., Li, X.Z., Zhang,
464 H.B., 2021. Effects of exotic *Spartina alterniflora* invasion on soil phosphorus and
465 carbon pools and associated soil microbial community composition in coastal
466 wetlands. *ACS Omega* 6(8), 5730–5738. <https://doi.org/10.1021/acsomega.0c06161>

467 Wang, Y.D., Wang, Z.L., Zhang, Q.Z., Hu, N., Li, Z.F., Lou, Y.L., Li, Y., Xue, D.M.,
468 Chen, Y., Wu, C.Y., Zou, C.B., Kuzyakov, Y., 2018. Long-term effects of nitrogen

469 fertilization on aggregation and localization of carbon, nitrogen and microbial
470 activities in soil. *Sci. Total Environ.* 624, 1131–1139.
471 <https://doi.org/10.1016/j.scitotenv.2017.12.113>

472 Wan, S.A., Mou, X.J., Liu, X.T., 2018. Effects of reclamation on soil carbon and
473 nitrogen in coastal wetlands of Liaohe River Delta, China. *Chinese Geogr. Sci.*
474 28(3), 443–455. <https://doi.org/10.1007/s11769-018-0961-7>

475 Wang, W.Q., Sardans, J., Wang, C., Zeng, C.S., Tong, C., Chen, G.X., Huang, J.F., Pan,
476 H., Peguero, G., Vallicrosa, H., Peñuelas, J., 2019. The response of stocks of C, N,
477 and P to plant invasion in the coastal wetlands of China. *Global Change Biol.* 25(2),
478 733–743. <https://doi.org/10.1111/gcb.14491>

479 Wu, H.B., Guo, Z.T., Gao, Q., Peng, C.H., 2009. Distribution of soil inorganic carbon
480 storage and its changes due to agricultural land use activity in China. *Agr. Ecosyst.*
481 *Environ.* 129, 413–421. <https://doi.org/10.1016/j.agee.2008.10.020>

482 Xia, S., Wang, W.Q., Song, Z.L., Kuzyakov, Y., Guo, L.D., Van Zwieten, L., Li, Q.,
483 Hartley, I.P., Yang, Y.H., Wang, Y.D., Andrew Quine, T., Liu, C.Q., Wang, H.L.,
484 2021. *Spartina alterniflora* invasion controls organic carbon stocks in coastal marsh
485 and mangrove soils across tropics and subtropics. *Global Change Biol.* 27(8),
486 1627–1644. <https://doi.org/10.1111/gcb.15516>

487 Xie, R.R., Zhu, Y.C., Li, J.B., Liang, Q.Q., 2019. Changes in sediment nutrients
488 following *Spartina alterniflora* invasion in a subtropical estuarine wetland, China.
489 *Catena* 180, 16–23. <https://doi.org/10.1016/j.catena.2019.04.016>

490 Xiang, J., Liu, D.Y., Ding, W.X., Yuan, J.J., Lin, Y.X., 2015. Invasion chronosequence
491 of *Spartina alterniflora* on methane emission and organic carbon sequestration in a
492 coastal salt marsh. *Atmos. Environ.* 112, 72–80.
493 <http://dx.doi.org/10.1016/j.atmosenv.2015.04.035>

494 Xu, X., Wei, S.J., Chen, H.Y., Li, B., Nie, M., 2022. Effects of *Spartina invasion* on the
495 soil organic carbon content in salt marsh and mangrove ecosystems in China. *J.*
496 *Appl. Ecol.* 00, 1–10. <https://doi.org/10.1111/1365-2664.14202>

497 Yang, P., Tang, K.W., Yang, H., Tong, C., Yang, N., Lai, D.Y.F., Hong, Y., Ruan, M.J.,
498 Tan, Y.Y., Zhao, G.H., Li, L., Tang, C., 2022a. Insights into the farming-season
499 carbon budget of coastal earthen aquaculture ponds in southeastern China. *Agr.*
500 *Ecosyst. Environ.* 335, 107995. <https://doi.org/10.1016/j.agee.2022.107995>

501 Yang, P., Tang, K.W., Tong, C., Lai, D.Y.F., Wu, L.Z., Yang, H., Zhang, L.H., Tang, C.,
502 Hong, Y., Zhao, G.H., 2022b. Changes in sediment methanogenic archaea
503 community structure and methane production potential following conversion of
504 coastal marsh to aquaculture ponds. *Environ. Pollut.* 305, 119276.
505 <https://doi.org/10.1016/j.envpol.2022.119276>

506 Yang, W., Zhao, H., Leng, X.L., Cheng, X., An, S.Q., 2017a. Soil organic carbon and
507 nitrogen dynamics following *Spartina alterniflora* invasion in a coastal wetland of
508 eastern China. *Catena* 156, 281–289. <https://doi.org/10.1016/j.catena.2017.03.021>

509 Yang, P., Bastviken, D., Jin, B.S., Mou, X.J., Tong, C., 2017b. Effects of coastal marsh
510 conversion to shrimp aquaculture ponds on CH₄ and N₂O emissions. *Estuar. Coast.*
511 *Shelf S.* 199, 125–131. <https://doi.org/10.1016/j.ecss.2017.09.023>

512 Yang, P., Zhang, L.H., Lai, D.Y.F., Yang, H., Tan, L.S., Luo, L.J., Tong, C., Hong, Y.,
513 Zhu, WY., Tang, K.W., 2022. Landscape change affects soil organic carbon
514 mineralization and greenhouse gas production in coastal wetlands. *Global*
515 *Biogeochem. Cy.* 36(12), e2022GB007469. <https://doi.org/10.1029/2022GB007469>

516 Yin, S., Bai, J.H., Wang, W., Zhang, G.L., Jia, J., Cui, B.S., Liu, X.H., 2019. Effects of
517 soil moisture on carbon mineralization in floodplain wetlands with different
518 flooding frequencies. *J. Hydrol.* 574, 1074–1084.
519 <https://doi.org/10.1016/j.jhydrol.2019.05.007>

520 Yuan, J.J., Xiang, J., Liu, D.Y., Kang, H., He, T.H., Kim, S., Lin, Y.X., Freeman, C.,
521 Ding, W.X., 2019. Rapid growth in greenhouse gas emissions from the adoption of
522 industrial-scale aquaculture. *Nat. Clim. Change* 9(4), 318–322.
523 <https://doi.org/10.1038/s41558-019-0425-9>

524 Zhang, D.H., Hu, Y.M., Liu, M., Chang, Y., Yan, X.L., Bu, R.C., Zhao, D.D., Li, Z.M.,
525 2017. Introduction and spread of an exotic plant, *Spartina alterniflora*, along
526 coastal marshes of China. *Wetlands* 37, 1181–1193.
527 <https://doi.org/10.1007/s13157-017-0950-0>

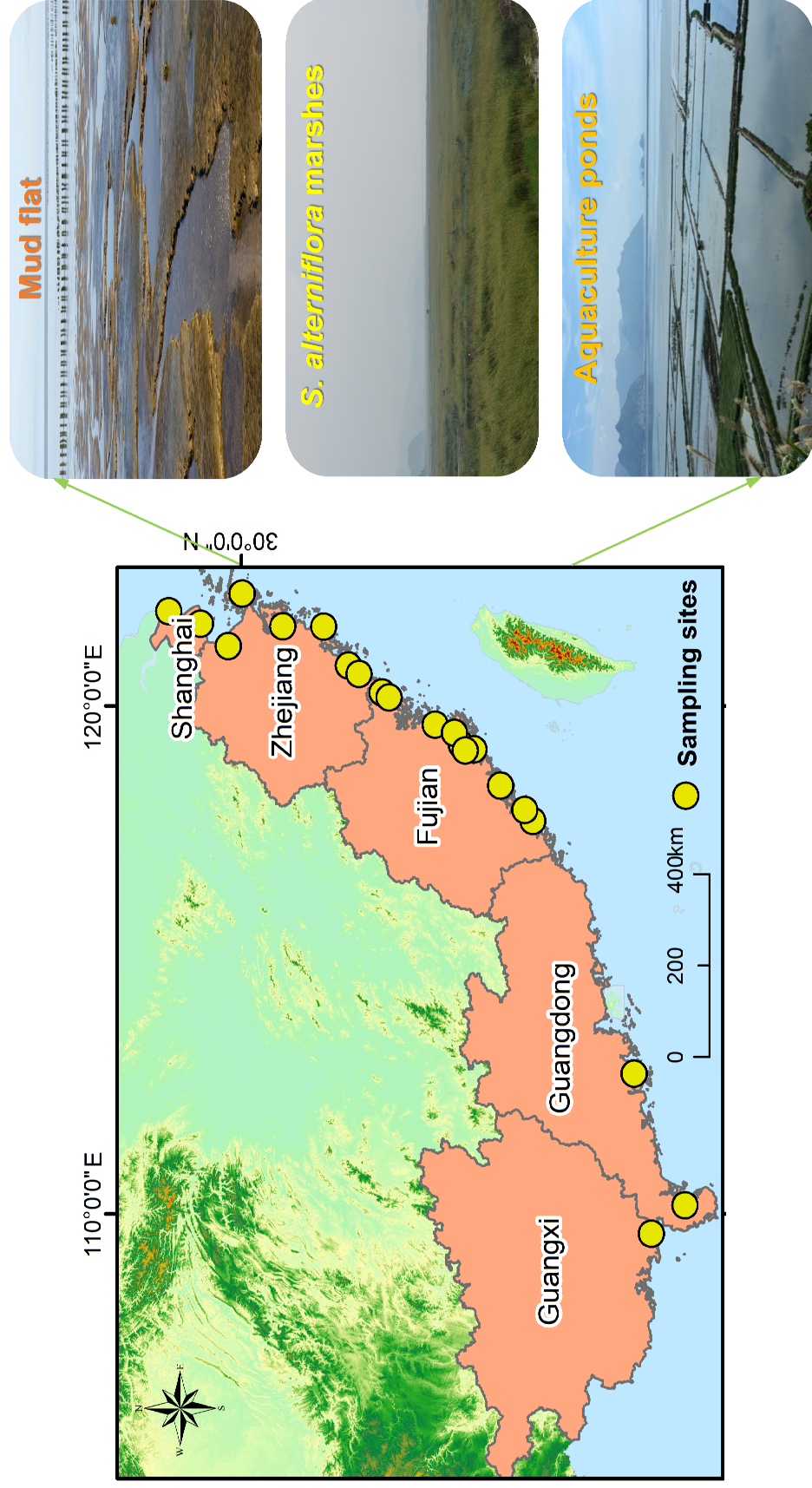
528 Zhang, G.L., Bai, J.H., Zhao, Q.Q., Jia, J., Wang, X., Wang, W., Wang, X.Y., 2021a.
529 Soil carbon storage and carbon sources under different *Spartina alterniflora*
530 invasion periods in a salt marsh ecosystem. *Catena* 196, 104831.
531 <https://doi.org/10.1016/j.catena.2020.104831>

- 532 Zhang, X.H., Zhang, Z.S., Li, Z., Li, M., Wu, H.T., Jiang M., 2021b. Impacts of
533 *Spartina alterniflora* invasion on soil carbon contents and stability in the Yellow
534 River Delta, China. *Sci. Total Environ.* 775, 145188.
535 <https://doi.org/10.1016/j.scitotenv.2021.145188>
- 536 Zhang, Y.H., Ding, W.X., Luo, J.F., Donnison, A., 2010. Changes in soil organic carbon
537 dynamics in an Eastern Chinese coastal wetland following invasion by a C₄ plant
538 *Spartina alterniflora*. *Soil Biol. Biochem.* 42, 1712–1720.
539 <https://doi.org/10.1016/j.soilbio.2010.06.006>
- 540 Zhu, T.T., Dittrich, M., 2016. Carbonate precipitation through microbial activities in
541 natural environment, and their potential in biotechnology: A review. *Front. Bioeng.*
542 *Biotech.* 4(4), <https://doi.org/10.3389/fbioe.2016.00004>
- 543 Zhu, Y.S., Wang, Y.D., Guo, C.C., Xue, D.M., Li, J., Chen, Q., Song, Z. L., Lou, Y.L.,
544 Kuzyakov, Y., Wang, Z.L., Jones, D.L., 2020. Conversion of coastal marshes to
545 croplands decreases organic carbon but increases inorganic carbon in saline soils.
546 *Land Degrad. Dev.* 31, 1099–1109. <https://doi.org/10.1002/ldr.3538>

Table 1

- 1 Regression equations for sediment organic carbon (SOC) and sediment inorganic carbon (SIC) contents as functions of sediment
- 2 physicochemical properties for the different habitat modification scenarios.

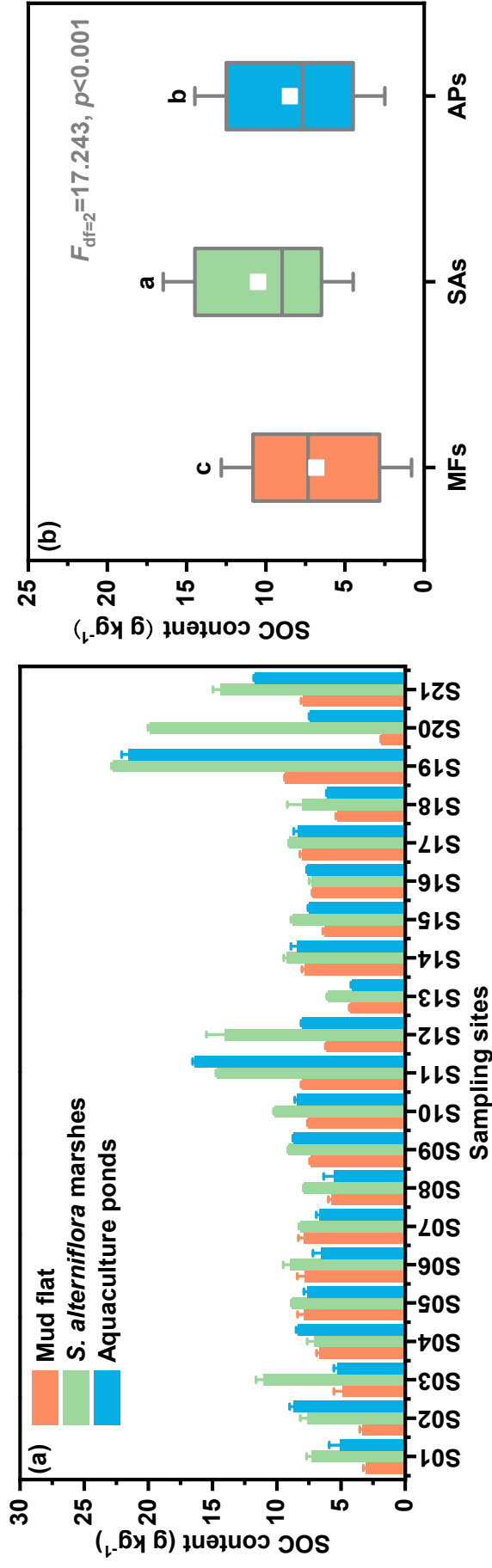
Habitat modification scenarios	Types	Regression equation	F value	R ²	p value
Conversion of MFs to SAs	SOC	$y = 15.419 + 0.180x_{\text{NH}_4^+ \text{-N}} - 1.227x_{\text{pH}}$	25.50	0.29	<0.001
	SIC	$y = 4.429 - 0.066x_{\text{NH}_4^+ \text{-N}} + 0.047x_{\text{Silt}} - 0.836x_{\text{Salinity}} + 0.053x_{\text{Cl}^-}$	11.10	0.27	<0.001
Conversion of SAs to APs	SOC	$y = 9.018 + 0.135x_{\text{NH}_4^+ \text{-N}} - 0.157x_{\text{SO}_4^{2-}} - 0.1595x_{\text{pH}}$	30.61	0.43	<0.001
	SIC	$y = 6.121 - 0.038x_{\text{Cl}^-} - 0.061x_{\text{NH}_4^+ \text{-N}} + 1.113x_{\text{NO}_3^- \text{-N}} - 0.065x_{\text{SO}_4^{2-}}$	19.93	0.40	<0.001



1

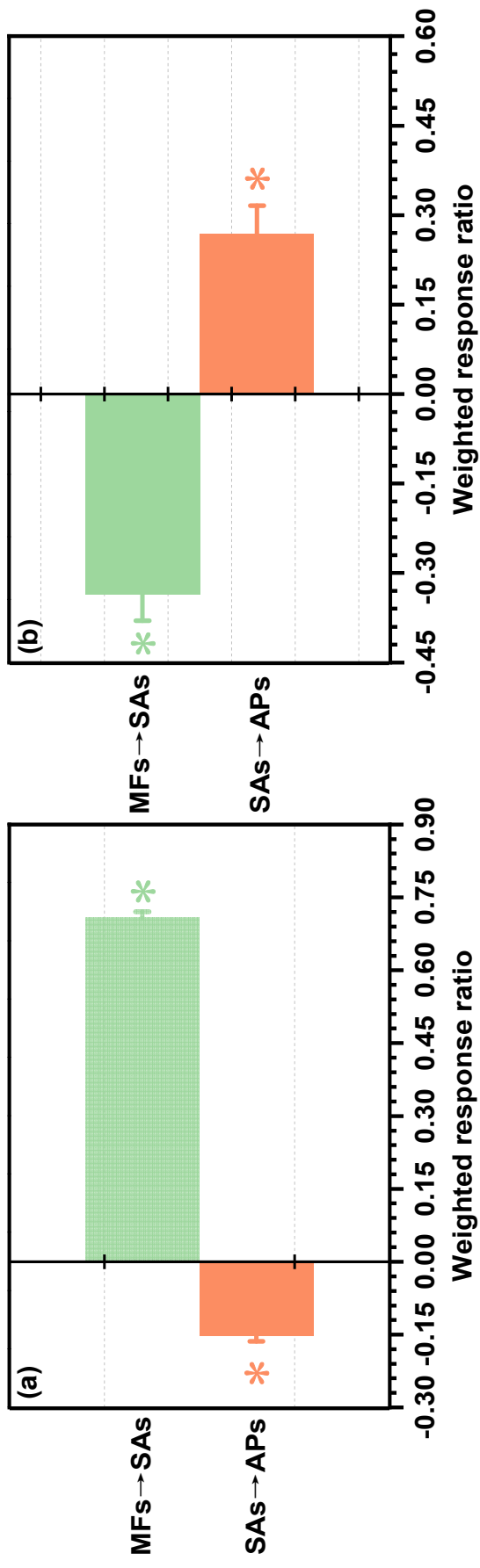
2 **Figure 1.** Locations of the 21 sampling sites across the coastal regions in southeastern China. Three wetland habitat types were

3 investigated including native mud flats (*MFs*), *S. alterniflora* marshes (*SAs*) and aquaculture ponds (*APs*).



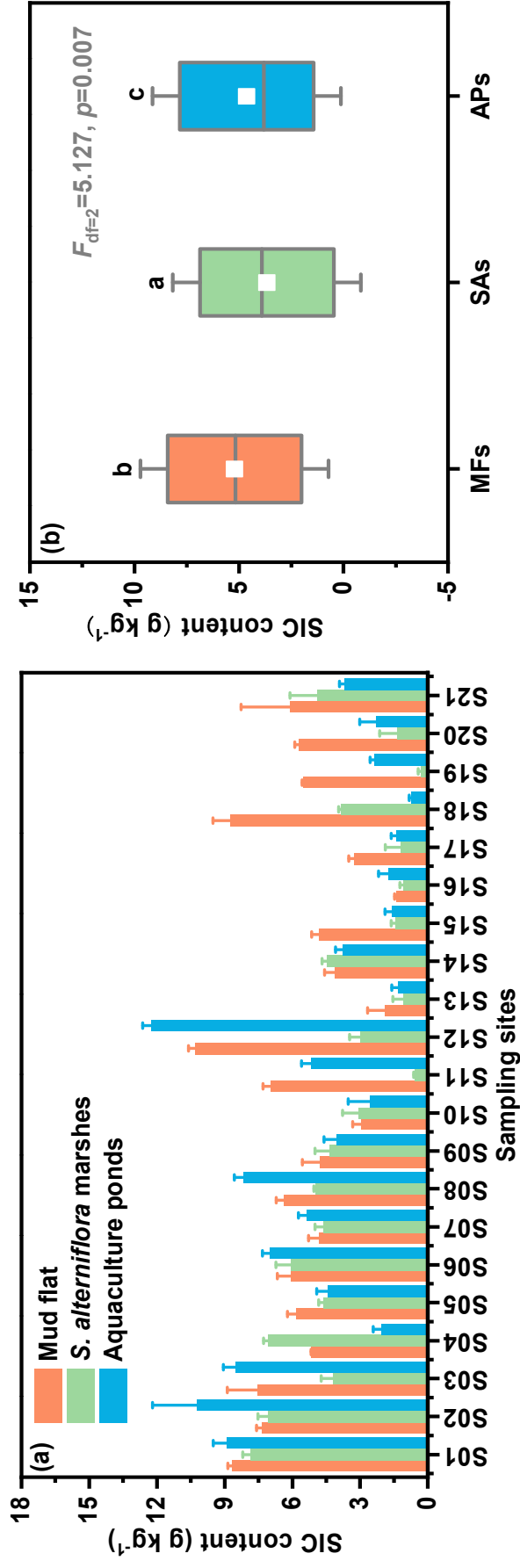
4

5 **Figure 2.** (a) surface sediment SOC content across three wetland habitat types for the 21 sampling sites, and (b) boxplots of surface sediment
6 SOC content for the three wetland habitat types. MFs, SAs and APs represent mud flats, *S. alterniflora* marshes and aquaculture ponds,
7 respectively. Different lowercase letters above the bars indicate significant differences between wetland habitat types ($p<0.05$). Error bars
8 represent standard error ($n = 63$).



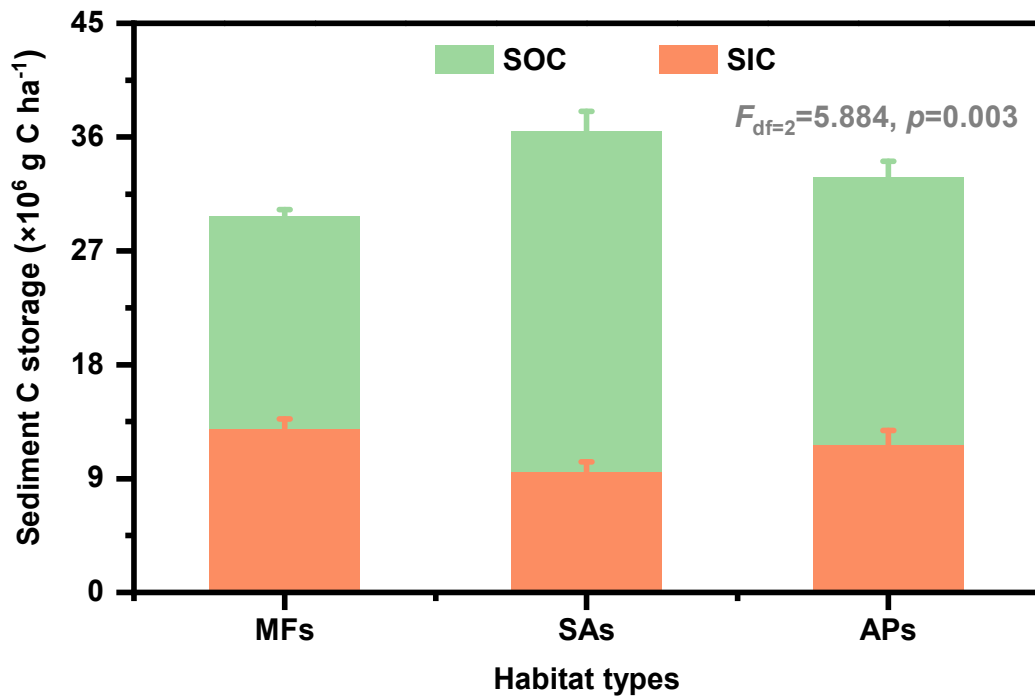
9

10 **Figure 3.** Weighted response ratios (RR++) of (a) SOC content, and (b) SIC content for the different habitat modification scenarios:
 11 MFs → SAs represents conversion of mudflats to *S. alterniflora* marshes; SAs → APs represents conversion of *S. alterniflora* marshes to
 12 aquaculture ponds. Bars represent the RR++ values and 95% CIs ($n = 63$). The asterisks (*) indicate significance at $p < 0.05$.



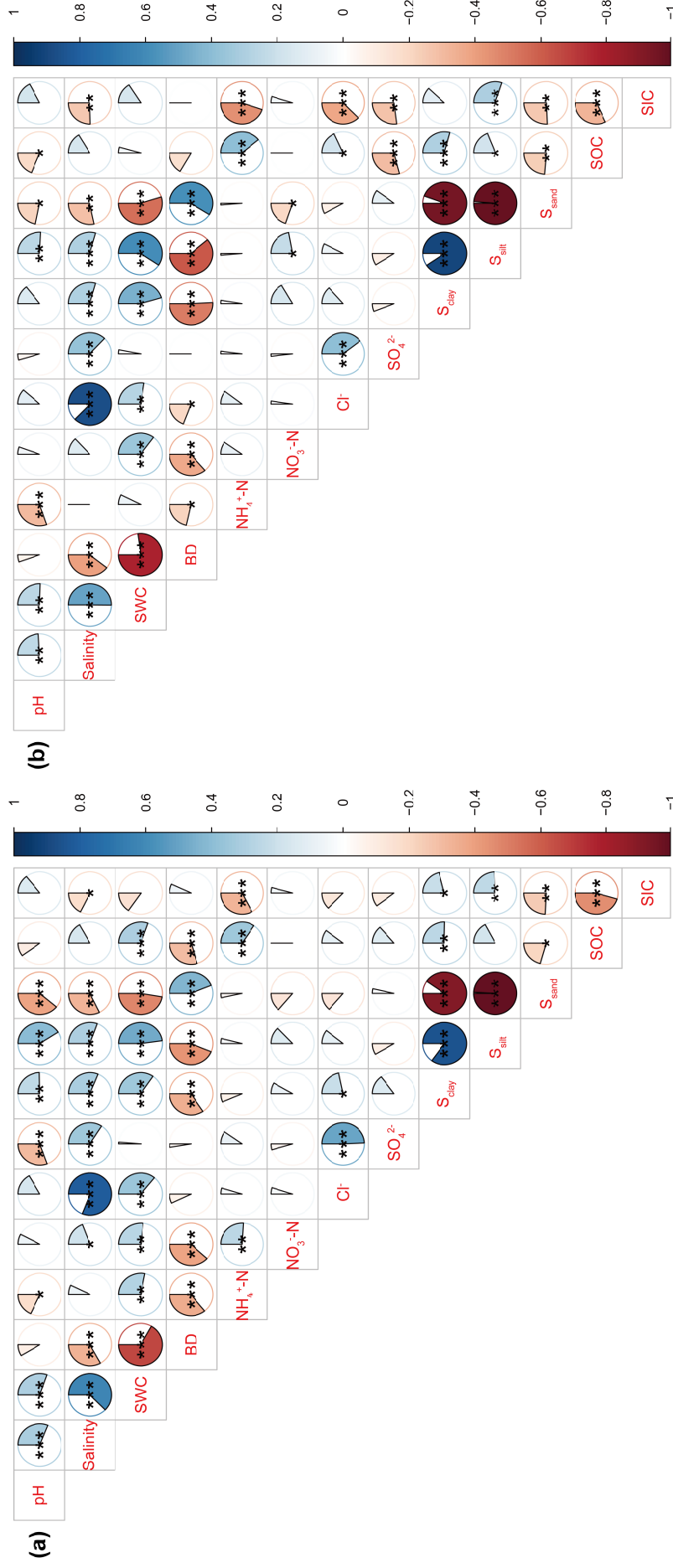
13

14 **Figure 4.** (a) surface sediment SIC content across three wetland habitat types for the 21 sampling sites, and (b) boxplots of surface
 15 sediment SIC content for the three wetland habitat types. MFs, SAs and APs represent mud flats, *S. alterniflora* marshes and aquaculture
 16 ponds, respectively. Different lowercase letters above the bars indicate significant differences between wetland habitat types ($p < 0.05$).
 17 Error bars represent standard error ($n = 63$).



18

19 **Figure 5.** Sediment storage of total C, sediment organic carbon (SOC), and
 20 sediment inorganic carbon (SIC) at 0-20 cm depth for the three wetland habitat
 21 types. MFs, SAs and APs represent mud flats, *S. alterniflora* marshes and
 22 aquaculture ponds, respectively. Error bars represent standard error ($n = 63$).



23

24 **Figure 6.** Correlation matrix for the different habitat modification scenarios: (a) conversion of MFs to SAs; (b) conversion of SAs to APs.

25 Colors of the circle segments indicate the direction of correlation (blue = positive; red = negative); size of the colored segment is proportional to

26 the r value (between -1 and 1). Asterisks within each circle indicate level of significance ($*p < 0.05$; $**p < 0.01$; $***p < 0.001$). SWC, BD, S_{clay} ,

27 S_{silt} , S_{sand} , SOC and SIC represent sediment water content, bulk density, clay content, silt content, sandy content, organic carbon and inorganic

28 carbon, respectively

1 **Supporting Information**

2 **Responses of coastal sediment organic and inorganic carbon to**
3 **habitat modification across a wide latitudinal range in**
4 **southeastern China**

5 Yan Hong^{a,b}, Linhai Zhang^{a,b,c}, Ping Yang^{a,b,c*}, Chuan Tong^{a,b,c}, Yongxin Lin^{a,b,c}, Derrick
6 Y. F. Lai^d, Hong Yang^{e,f}, Yalian Tian^{a,b}, Wanyi Zhu^{a,b}, Kam W. Tang^{g*}

7 ^a*School of Geographical Sciences, Fujian Normal University, Fuzhou 350007, P.R.*
8 *China,*

9 ^b*Key Laboratory of Humid Subtropical Eco-geographical Process of Ministry of*
10 *Education, Fujian Normal University, Fuzhou 350007, P.R. China*

11 ^c*Research Centre of Wetlands in Subtropical Region, Fujian Normal University, Fuzhou*
12 *350007, P.R. China*

13 ^d*Department of Geography and Resource Management, The Chinese University of Hong*
14 *Kong, Shatin, New Territories, Hong Kong SAR, China*

15 ^e*College of Environmental Science and Engineering, Fujian Normal University, Fuzhou,*
16 *350007, China*

17 ^f*Department of Geography and Environmental Science, University of Reading, Reading,*
18 *RG6 6AB, UK*

19 ^g*Department of Biosciences, Swansea University, Swansea SA2 8PP, U. K.*

20
21 ***Correspondence to:**

22 Ping Yang (yangping528@sina.cn); Kam W. Tang (k.w.tang@swansea.ac.uk)

23 **Telephone:** 086-0591-87445659 **Fax:** 086-0591-83465397

24 **Supporting Information Summary**

25 **No. of pages: 4** **No. of tables: 1**

26 **Page S3:** Table S1. Fitting parameters of the first order kinetics for soil organic carbon
27 mineralization in surface soil (0–20 cm) from three wetland habitat types across the
28 different coastal sites in China.

29 **Table S1** Surface soil physico-chemical properties across the three wetland habitat types.
 30 MFs, SAs and APs represent mud flats, *S. alterniflora* marshes and aquaculture ponds,
 31 respectively.

Sediment physiochemical properties	Habitat types		
	MFs	SAs	APs
pH	7.99±0.06a	7.95±0.06a	7.82±0.06a
Salinity (‰)	3.96±0.20a	4.54±0.23a	4.21±0.31a
SWC (%)	43.05±1.33b	47.12±1.38a	47.78±1.70a
BD (g cm ⁻³)	1.29±0.02a	1.26±0.02a	1.25±0.03a
NH ₄ ⁺ -N (mg kg ⁻¹)	13.32±1.37c	24.01±2.18a	16.85±1.78b
NO ₃ ⁻ -N (mg kg ⁻¹)	1.25 ± 0.05b	1.85±0.16a	1.45±0.13b
Cl ⁻ (mg L ⁻¹)	36.84±2.15b	40.94±2.23a	37.75±3.43b
SO ₄ ²⁻ (mg L ⁻¹)	8.90±0.63b	9.13±0.50b	17.48±1.40a
<i>Soil particle size composition</i>			
Clay (%)	10.41±0.47a	10.94±0.49a	10.50±0.57a
Silt (%)	54.07±2.29a	52.67±2.41bc	50.14±2.56c
Sandy (%)	35.53±2.69b	36.38±2.86b	39.35±3.06a

32 Lowercase letters within the same column indicate significant differences at $p < 0.05$ between three
 33 wetland habitat types. Data are after [Yang et al. \(2022\)](#) for reference and review only. See main text for
 34 explanation of the abbreviations.

35 **References**

- 36 Yang, P., Zhang, L.H., Lai, D.Y.F., Yang, H., Tan, L.S., Luo, L.J., Tong, C., Hong, Y.,
37 Zhu, W.Y., Tang, K.W., 2022. Landscape change affects soil organic carbon
38 mineralization and greenhouse gas production in coastal wetlands. *Global Biogeochem.*
39 *Cy.* 36(12), e2022GB007469. <https://doi.org/10.1029/2022GB007469>